K., Crouch, R., Yudd, A., and Nakanishi, K. (1975), *Biochemistry 14,* 3933.
Fenstermacher, P. R., and Callender, R. H. (1974), *Opt. Commun. 10,* 181.
Gilardi, R. D., Karle, I. L., and Karle, J. (1972), *Acta Crystallogr. Sect. B 28,* 2605.
Gill D., Heyde, M. E., and Rimai, L. (1971), *J. Am. Chem. Soc. 93,* 6288.
Heyde, M. E., Gill, D., Kiponen, R. G., and Rimai, L. (1971), *J. Am. Chem. Soc. 93,* 6776.
Honig, B., and Ebrey, T. G. (1974), *Annu. Rev. Biophys. Bioeng, 3,* 151.
Honig, B., and Karplus, M. (1971), *Nature (London) 229,* 558.
Landau, L. D., and Lifshitz, E. M. (1959), Fluid Mechanics, London, Pergamon Press, Chapter 2.
Lewis, A., Fager, R. S., and Abrahamson, E. W. (1973), *J. Raman Spectrosc. 1,* 465.
Lewis, A., Spoonhower, J., Bogomoin, R. A., Lozier, R. H., and Stoeckenius, W. (1974), *Proc. Natl. Acad. Sci., U.S.A. 71,* 4462.
Mathies, R., Oseroff, A. R., and Stryer, L. (1976), *Proc. Natl. Acad. Sci. U.S.A. 73,* 1.
Mendelsohn, R. (1973), *Nature (London) 243,* 22.
Mendelsohn, R., Verma, A. L., Berstein, H. J., and Kates, M. (1974), *Can. J. Biochem. 52,* 774.
Oseroff, A. R., and Callender, R. H. (1974), *Biochemistry 13,* 4243.
Papermaster, D. S., and Dreyer, W. J. (1973), *Biochem. 13,* 2438.
Rimai, L., Gill, D., and Parsons, J. L. (1971), *J. Am. Chem. Soc. 93,* 1353.
Rowan, R., Warshel, A., Sykes, B. D., and Karplus, M. (1974), *Biochemistry 13,* 970.
Tang, J., and Albrecht, A. C. (1970), Raman Spectroscopy 2, Chapter 2.
Tennekes, H., and Lumley, J. L. (1972), A First Course in Turbulence, Cambridge, Mass., MIT Press, Chapter 5.
Wald, G. (1967), *Science 162,* 230.
Wald, G. (1968), *Nature (London) 219,* 800.
Warshel, A., and Karplus, M. (1974), *J. Am. Chem. Soc. 96,* 5677.

Reaction Free Energy Surfaces in Myosin–Actin–ATP Systems†

Terrell L. Hill* and Evan Eisenberg

ABSTRACT: If we select for consideration any reaction $M_1 \rightleftarrows M_2$ in the myosin-ATPase cycle, the question arises as to the relations between the rate constants for (1) $M_1 \rightleftarrows M_2$, (2) $AM_1 \rightleftarrows AM_2$ (A = actin), (3) $A + M_1 \rightleftarrows AM_1$, and (4) $A + M_2 \rightleftarrows AM_2$, with actin and myosin either (a) in solution or (b) in the myofilament structure. It is shown here, by means of examples, that a single so-called potential of mean force, W, and structural free energy, A_m, suffice to determine the reaction free energy surfaces for all of these transitions (W for the solution case, $W + A_m$ for the structured case). In fact, A_m is the same for all reactions in the myosin-ATPase cycle. Of course, though indispensable as the starting point and adequate for qualitative understanding, the reaction free energy surface does not provide (without additional theory) the actual values of the rate constants or of the corresponding basic free energy changes in the myosin states involved. These rate constants and free energies are discussed, in a preliminary way, in two other papers.

The kinetics of myosin-ATPase activity is important because of its relation to muscle contraction. This relation is also responsible for the complexity of the subject: myosin-ATPase activity is considerably altered either in the presence of actin in solution or when its locale is the myofilament system of active muscle. From the theoretical side, the first step in trying to understand some of these complications is to visualize the transitions of the myosin-ATPase cycle in terms of reaction free energy surfaces (analogous to the potential surfaces of molecular rate theories). The object of this paper is to discuss the pertinent free energy surfaces in the simplest possible terms, basing the argument on rather arbitrary examples chosen for illustrative purposes only. Our aim is to sketch the essential features involved; the details and choice of examples will certainly need to be altered in the future as more biochemical and structural information becomes available.

In two other papers (T. L. Hill, manuscript in preparation; 1975a), the argument given here will be supplemented in more quantitative terms. This elaboration will include a preliminary discussion of the connections between the reaction free energy surfaces, on the one hand, and the corresponding rate constants and basic free energy levels (Hill and Simmons, 1976) of myosin states, on the other. To put it briefly, contributions must be considered, *other than* from the reaction free energy surface, to both the basic free energies and the activation free energies (see also Hill, 1976).

The present paper is concerned only with free energy surfaces per se. However, these surfaces are the most important single feature involved and are adequate to provide a qualitative understanding of the problem.

† From the Laboratory of Molecular Biology, National Institute of Arthritis, Metabolism, and Digestive Diseases (T.L.H.), and the Laboratory of Cell Biology, National Heart and Lung Institute (E.E.), National Institutes of Health, Bethesda, Maryland 20014. *Received October 6, 1975.*

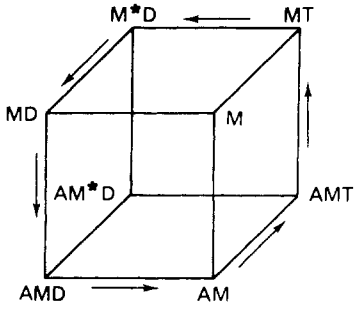

FIGURE 1: States and transitions in the biochemical kinetic diagram of myosin (S1) + actin + ATP. Each line represents both forward and backward transitions. See text. Arrows denote the presumed most important cycle. The figure applies both to S1 in solution and to S1 in the myofilament system.

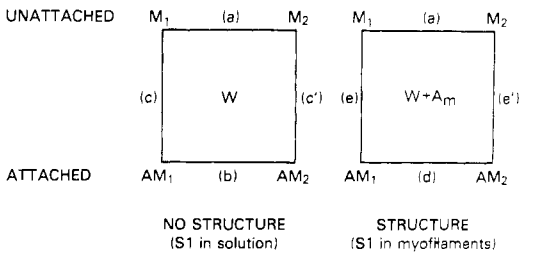

FIGURE 2: One of the vertical squares taken from the diagram in Figure 1, without and with myofilament structure. See text for meaning of W and A_m.

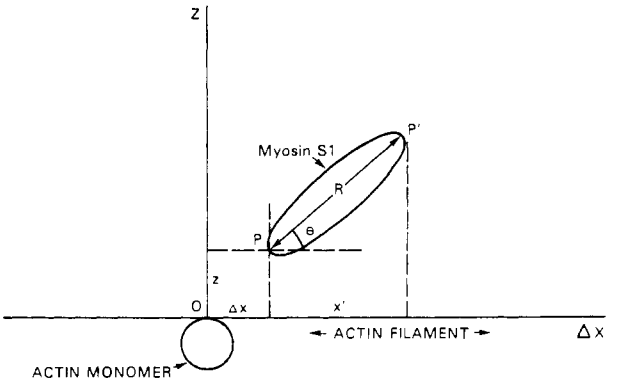

FIGURE 3: Coordinates relating position of S1 to actin site. See text.

There are two principal sorts of application of these considerations, the first biochemical and the second biophysical: (1) to help understand the interrelations between sets of rate constants of the myosin-ATPase cycle (a) in the absence of actin, (b) in the presence of actin, and (c) in the structured myofilament system; and (2) as an aid in the rational (as opposed to empirical) selection of rate constants in explicit models of muscle action. A theoretical approach may be especially helpful in studies on the structured system since many of the rate constants of this system are x dependent (Hill, 1974, 1975b; see also Figure 7, below) yet experiments (mechanical transients, noise, etc.) can give only x-averaged results.

We use as a starting point many of the qualitative ideas summarized by Huxley (1969) and Huxley and Simmons (1971, 1973).

1. The Biochemical Diagram

For concreteness and simplicity in our discussion, we condense the actual myosin-ATPase cycle in solution (Lymn and Taylor, 1971; Eisenberg and Kielley, 1973; Bagshaw et al., 1974) down to a hypothetical four-state cycle M → MT → M*D → MD →, where M = S1 moiety of myosin, T = ATP, D = ADP, P_i, and M*D denotes M in some different molecular structure (conformation) than in MD. In the presence of F-actin (in solution), four additional states (actin-bound or "attached", as we shall call them) are possible, as indicated in the "diagram" (Hill, 1974) in Figure 1, where A = actin. For orientation, the arrows in the figure show the presumed dominant cycle.

A myosin state that is stable in the unattached cycle (upper square) may possibly lose its stability when S1 is attached to actin, or vice versa.

In the structured (myofilament) systems, the corresponding diagram still appears formally as in Figure 1, but the rate constants associated with the vertical lines (attachment-detachment) and with the lower (attached) square are not only expected to be different from those in solution but are, in general, x dependent (Hill, 1974). The rate constants in the upper (unattached) square can reasonably be assumed to be the same (under the same ionic and other conditions) whether the S1 is free in solution or is in the myofilament lattice (linked to S2, etc.). The introduction of structure may destabilize an attached state or may create a new state. Examples will be mentioned below.

For purposes of analysis, the basic unit in Figure 1 is *any* pair of neighboring myosin states in the unattached cycle (call them M_1 and M_2 for generality), the corresponding attached states AM_1 and AM_2, and the transitions (lines) connecting these four states. These vertical "panels" (one for the free S1 case, one for the structured case), abstracted from Figure 1, are shown in Figure 2. Our objective in this paper is to discuss in a qualitative way the reaction free energy surfaces that are fundamental for an understanding of the connections between rate constants (and free energies of states) for the various transitions (a), (b), . . . , (e') in Figure 2.

2. The Potential of Mean Force (Reaction Free Energy)

In the theory of reaction kinetics between atoms, a quantum mechanical potential surface plays a key role. This is the ground-state electronic energy as a function of the configuration of the nuclei. Here we deal with large molecules (M, T, etc.) in the presence of a multicomponent solvent. The corresponding quantity is a potential of mean force W, obtained by appropriate statistical mechanical averaging (Hill, 1956, 1960, 1975a, 1976).

At this point we introduce some of the needed coordinates. Figure 3 shows an S1 molecule in solution in a fixed configuration relative to a particular attachment site, at the origin O, on the actin filament. The complementary site on S1 is at P. P is displaced an arbitrary (radial) distance z away from the actin filament and a longitudinal distance Δx from the actin site. The tilt of S1 is measured by θ or, alternatively, by $x' = R \cos\theta$ ($-R \leq x' \leq +R$), where $R \simeq 150$ Å (Moore et al., 1970). The so-called "rigor" angle is $\theta \simeq 45°$. Other, less important, coordinates are of course also involved (Hill, 1975a), but for present purposes they are considered fixed at their optimal values (i.e., such as to minimize W).

The progress of the two transitions 1 ⇄ 2 (Figure 2), for any fixed position Δx, z, x' of M relative to A (i.e., from M unattached to attached), may be followed by another coordinate s. In the case of an "isomeric" change (e.g., MT ⇄

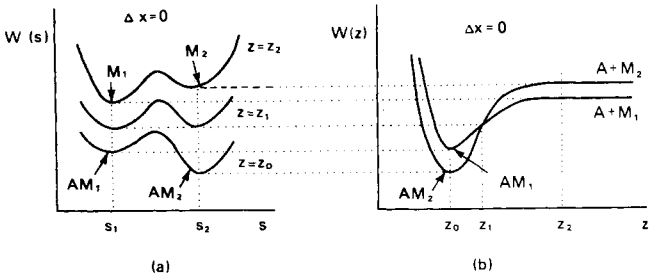

FIGURE 4: (a) Reaction free energy W, in an example, as a function of the coordinate s for three different distances (z) of S1 from the actin site. See text. (b) W as a function of z for the two states 1 and 2. See text.

M*D or M*D ⇄ MD in Figure 1), s would be the so-called reaction coordinate (i.e., along the path of minimum potential energy) in the (quantum-mechanical) potential surface for the particular transition (Hill, 1960). In the case of binding or release of a ligand (e.g., M + T ⇄ MT or M + D ⇄ MD in Figure 1), the reaction coordinate s would be the distance of the ligand from its binding site on M (analogous to z in Figure 3). In both cases, additional coordinates would be needed (T. L. Hill, manuscript in preparation; 1975a, 1976) to describe the complete potential surface involved.

There are four vertical panels in Figure 1 (Figure 2 represents only one of them). Each of these would have its own s variable, depending on the nature of the transition.

W, the potential of mean force for this reaction (1 ⇄ 2), is the free energy of one S1 molecule (and one ligand molecule in a binding transition) in a fixed position Δx, z, x' relative to the actin site and at a fixed extent of reaction s, statistically averaged (Hill, 1956, 1960) over all possible configurations of all solvent molecules and over the rotational coordinates of the ligand (if there is one) at s. Thus, in this simplified discussion, W is a function of Δx, z, x', and s. As to physical significance, the negative derivative of W with respect to one of the coordinates on which it depends gives the statistically averaged force tending to displace the system along the given coordinate (Hill, 1956, 1960). For brevity, we shall usually refer to W as the reaction free energy or even as a free energy.

3. S1 in Solution (The Unstructured System)

In the absence of structural restraints, S1 is free to approach the actin site as it pleases, so to speak. Therefore in this section, to further simplify, we consider approaches only along the optimal path $\Delta x = 0$ (i.e., point P, Figure 3 is always on the Z axis). The remaining variables are then z, x', and s.

An explicit example, based on Figure 2, is shown in Figures 4 and 5. We suppose here that 1 ⇄ 2 is an isomeric reaction with state 1 somewhat more stable (in terms of W) than state 2 when z is large (i.e., M_1 is more stable than M_2). But M_2 is attached more strongly to actin than is M_1, with the consequence that AM_2 is more stable than AM_1. In both cases, we assume, $z = z_0$ is the value of z that provides strongest attachment of S1 to the actin site. The scale of z in Figure 4b is such that $z_2 - z_0$ is of order 10 Å. The optimal values of s in the two states, s_1 and s_2, are assumed to be independent of z. M_1 attaches to actin at an optimal angle of $\theta = 90°$ ($x_1' = 0$) while M_2 attaches most strongly at $\theta = 45°$ ($x_2' = R/\sqrt{2}$).

The top curve in Figure 4a shows $W(s)$ for a large value

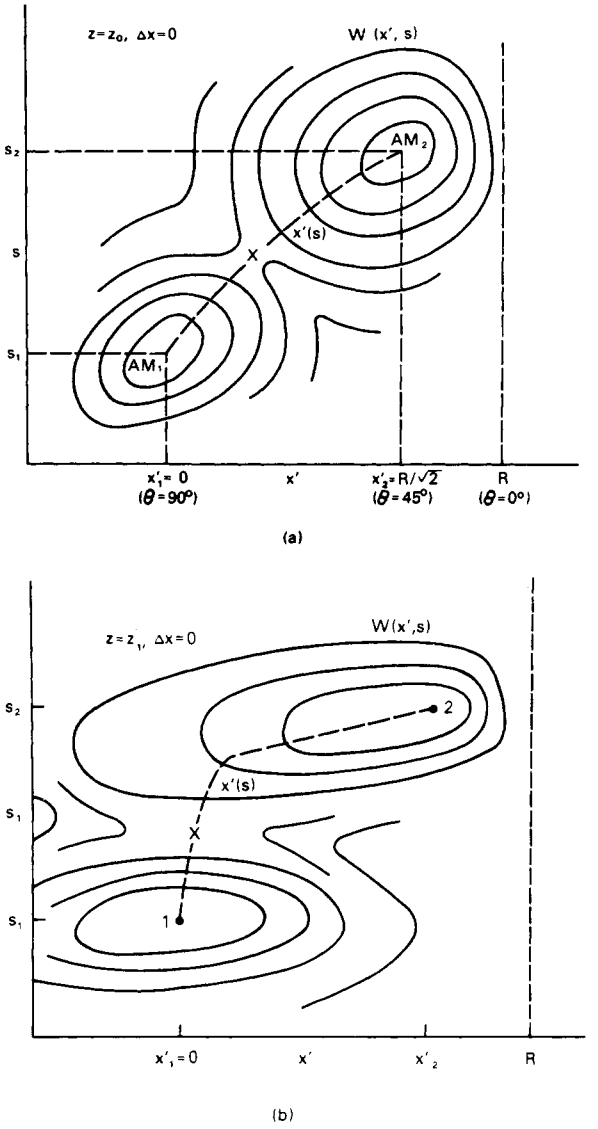

FIGURE 5: (a) Hypothetical contour map of $W(x',s)$, for AM_1 ⇄ AM_2 ($z = z_0$), in an example. See text for details. (b) $W(x',s)$ in the same example for a larger value of z, $z = z_1$. See text.

of z, $z = z_2$ (compare Figure 4b). When z is large, W becomes independent of both z and x'. This top curve in Figure 4a, then, represents W in the reaction M_1 ⇄ M_2 [(a) in Figure 2]. The minima (at s_1 and s_2) correspond to the two stable states. Incidentally, if 1 ⇄ 2 represented a myosin-ligand interaction, say MT ⇄ M + T, then $W(s)$ (top curve) might appear as modified by the dashed line. A free energy barrier to binding would be expected (Hill, 1975a) because of the loss of rotational freedom of T as it approaches the binding site on M (recall that statistical averaging over the rotational coordinates of the ligand is included in W). Also, there may be an electrostatic contribution to such a barrier.

Consider next the situation at $z = z_0$, that is, for the reaction AM_1 ⇄ AM_2 [(b) in Figure 2]. For this fixed z, W is a function of x' and s, shown schematically as a contour map in Figure 5a. The two basins at s_1, x_1', and s_2, x_2' (states AM_1 and AM_2) are connected by a saddle-point at X. The AM_2 basin is deeper than the AM_1 basin. The reaction path between the two states is designated by $x'(s)$. $W(s)$ along this path (with maximum at X) is shown as the bottom curve in Figure 4a.

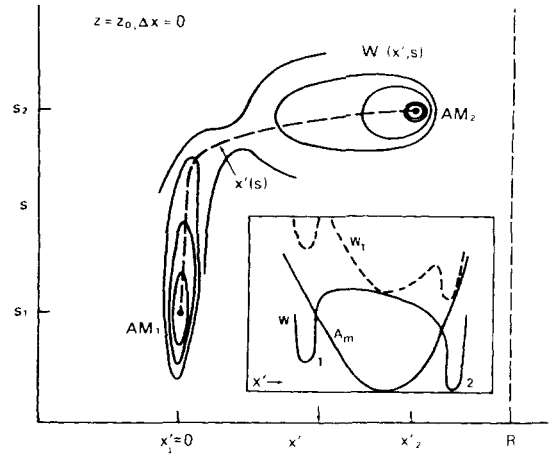

FIGURE 6: A different example of $W(x',s)$ at $z = z_0$. Compare Figure 5a. See text. The arrow on the abscissa is referred to under Possible Appearance of a New Attached State (section 4). Inset: see the same subsection in section 4.

It should be noted that the two scales in Figure 5a are quite different. Thus $x_2' - x_1'$ is of order 100 Å while $s_2 - s_1$ might involve for example, some internal structural movement in M of order, say, 5 Å. The contours used in Figure 5a imply that the angle θ is moderately flexible about both minima.

It is worth digressing to remark that this difference in scales, just mentioned, touches on the essence of sliding filament models of muscle contraction (Hill, 1974): one way or another, chemical changes on a scale of angstroms must be amplified into macromolecular movement on a scale of 100 Å or more. Figure 5a (see also Figures 6 and 8, below) illustrates, at the most fundamental level, this union of biochemistry and macromolecular mechanics. It also raises the question whether the chemical change occurs before, during, or after the macromolecular movement.

Figure 4b clarifies the connection between the $z = z_2$ and $z = z_0$ cases, above. In this figure we show W as a function of z with the approach (S1 to actin site) made at either s_1, x_1' or s_2, x_2'. That is, $W(z)$ in this figure shows the depth of the two basins as a function of z. These two $W(z)$ curves also represent W along the reaction path for the two attachment transitions [(c) and (c') in Figure 2]. Note the relations between W values in Figures 4a and 4b.

Figure 5b shows $W(x',s)$ at an intermediate value of z, $z = z_1$, where the two basins have the same depth. The middle curve in Figure 4a gives $W(s)$ along the reaction path $x'(s)$ for this case. Note that the free energy basins in Figure 5b are oriented more or less parallel to the x' axis; i.e., W is becoming relatively insensitive to x' (or θ). The corresponding contour map (not shown) for $z = z_2$ (or for any z in the plateau region of Figure 4b) would consist entirely of lines parallel to the x' axis. That is, the two basins would become valleys. A vertical section (x' = constant) through this map at any x' between $-R$ and R would give the top curve in Figure 4a.

Because we have seen in Figures 4 and 5 several different aspects of the reaction free energy surface for this example, it should perhaps be emphasized that there is in fact only a *single* function $W(z,x',s)$ that is fundamental for the determination of *all* of the eight rate constants in the left-hand panel of Figure 2.

Of course contour maps of the sort shown in Figure 5a may exhibit considerable variety. Another example is presented in Figure 6. Here, in the transition $AM_1 \rightarrow AM_2$, along $x'(s)$, the "chemical" change ($s_2 - s_1$) is largely completed before S1 tilts ($x_2' - x_1'$). Also, note that the angles $\theta = 90°$ and $\theta = 45°$ are quite inflexible, or specific, in the two free energy wells (states AM_1 and AM_2). This kind of specificity is of course typical of enzymatic behavior whereas the considerable angular (x' or θ) flexibility exhibited in Figure 5a is atypical. However the "typical" case presents a possible problem: the molecular elasticity that must reside *somewhere* in any sliding filament model of muscle function would have to come almost entirely from sources *other than* S1 tilt, e.g., from the length of S2 (see below).

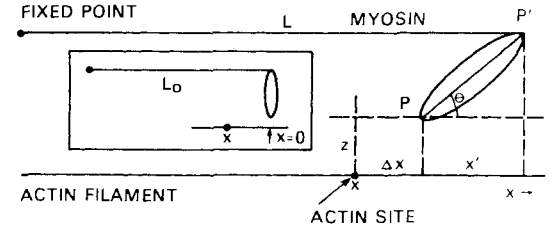

FIGURE 7: Schematic drawing of cross-bridge in structured system. See text. Inset: location of origin on x axis.

4. Myofilament S1 (The Structured System)

We now consider S1 attached to S2 in the myofilament system, as shown schematically in Figure 7. We ignore any "two-headed" complications since these are uncertain at present. For geometric simplicity, because it is relatively long, we take S2 to be parallel to the actin filament. The position of the actin site on the actin filament relative to some arbitrary fixed point on the cross-bridge of the myosin filament is specified by a new variable x (Hill, 1974), not to be confused with Δx already introduced. We assume that the transitions $M_1 \rightleftarrows M_2$ (Figure 2) and the interaction between S1 (point P) and the actin site are unaltered by the linkage of S2 and S1 at P'. In other words, we take the function $W(\Delta x,z,x',s)$ (we previously held $\Delta x = 0$) to be the same in the structured system as in the unstructured system. But there is a new contribution to the reaction free energy, which we denote by A_m: the total reaction free energy is now $W_t = W + A_m$.

While W takes into account internal transformations in S1 and the interaction of S1 (point P, Figure 7) with the actin site, the "structural" free energy A_m is associated with the interaction between S1 (point P') and the myosin filament (including S2). A_m could receive contributions from several sources, for example from the S1–S2 angle (the same as θ), the length of S2 (L), the region of insertion of the cross-bridge into the myosin filament, etc. In general, A_m might be a function of x, Δx, and x' (but not z, since S2 is assumed parallel to the actin filament).

Note that A_m depends on the variable x but W does not. Conversely, W depends on s but A_m does not. Consequently, A_m would be the same function regardless of which reaction $M_1 \rightleftarrows M_2$ in the myosin cycle is being considered.

The particular case we examine here is that A_m is a function of $L - L_0$ only (L_0 = equilibrium length of S2), for example, $A_m = K_L(L - L_0)^2/2$, where K_L is a force constant. That is, S2 behaves like a simple spring (Huxley and Simmons, 1971).

For convenience, we locate the origin $x = 0$ on the x axis

as shown in the inset of Figure 7, that is, at the point of contact between S1 and actin when $L = L_0$ and $\theta = 90°$. Then it follows that $L - L_0 = x + \Delta x + x'$. Thus, in this special case, A_m is a function of the sum $x + \Delta x + x'$ only, and A_m has its minimum value (taken as zero) when $L = L_0$, $x + \Delta x + x' = 0$.

Unattached and Attached Transitions. When z is large, the *unattached* transitions $M_1 \rightleftarrows M_2$ [(a) in Figure 2] occur in the same way and at the same rates whether there is structure or not. W degenerates in this special case into a function of s only and W_t becomes $W(s) + A_m(L - L_0)$, where $W(s)$ is again the top curve in Figure 4a. The two contributions to W_t do not "interact" (i.e., they do not depend on the same variables): $W(s)$ governs the rates of the transitions ($\rightleftarrows$) while A_m controls the equilibrium fluctuations in length L of S2.

We turn now to the *attached* reaction $AM_1 \rightleftarrows AM_2$ in the structured case [(d) in Figure 2]. This can be dealt with to a good approximation by again fixing $z = z_0$ and $\Delta x = 0$ as in the unstructured system (i.e., in spite of some perturbation induced by A_m, the optimal values of z and Δx will be $z \simeq z_0$ and $\Delta x \simeq 0$). In this case, then, $L - L_0 = x + x'$, A_m is a function of $x + x'$, and W becomes the same function of x' and s as shown in Figure 5a (to continue with the example introduced in section 3).

From $L - L_0 = x + x'$ we note that, with x held constant, x' can change only by changing L.

Figure 8 illustrates in a very schematic way the relations between W, A_m, and W_t for one particular value of x. The solid contour map is $W(x',s)$ from Figure 5a. The vertical lines represent the vertical free energy valley $A_m(x + x')$, with minimum ($L = L_0$, $A_m = 0$) at $x' = -x$ (darker vertical line). A horizontal section (s = constant), at any s, through A_m would show, for example, a parabola with curvature K_L. The dashed contours indicate (sketchily) the contour map of $W_t = W + A_m$ for this particular x. The dashed line is the reaction path from AM_1 to AM_2 (structured, at x). The minima of the two basins are shifted somewhat in position and are less deep than in the unstructured case [$W(x',s)$]. If another value of x is considered, $W(x',s)$ remains unchanged but the vertical valley A_m is translated to the right or left depending on the new value of x. Of course $W_t(x',s,x)$ will have a different appearance for each value of x. For some values of x, one or the other of the basins in W_t may disappear (i.e., these states may not be stable at all x).

Clearly, the x dependence of the rate constants between a pair of attached states, as used in models of muscle contraction (Hill, 1974), has its origin in the x dependence of the appropriate reaction free energy surface W_t, as illustrated here. Furthermore, we see here the source of the connection between the rate constants for $AM_1 \rightleftarrows AM_2$ with S1 in solution (based on W) and the corresponding rate constants for the structured system at specified x (based on $W_t = W + A_m$).

If S2 is almost inelastic (K_L large), as seems rather likely, then the vertical free energy valley at $x' = -x$ (Figure 8), A_m, will have very steep walls. In this case, $W_t = W + A_m$ will also appear as a vertical valley with steep walls at $x' = -x$. Furthermore, the free energy of this latter valley floor is determined by taking a vertical section (i.e., x' = constant) through $W(x',s)$ at $x' = -x$ (darker vertical line). That is, $W_t(s) \simeq W(-x,s)$ for a given fixed value of x. For the choice of x made in Figure 8, this $W_t(s)$ would have two minima (states AM_1 and AM_2) and a maximum

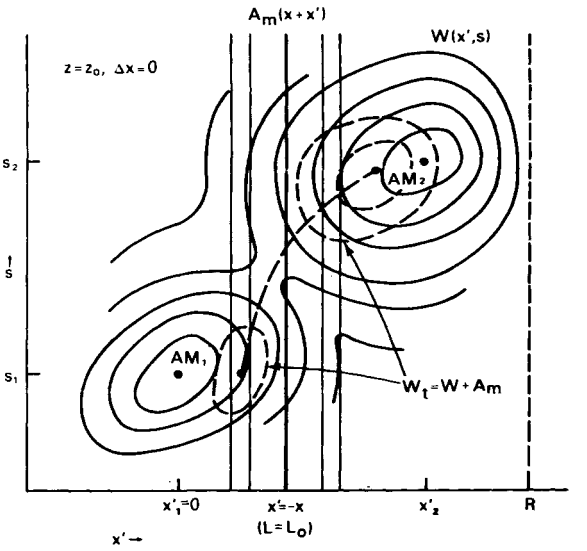

FIGURE 8: Illustration of construction of W_t (dashed contours) at $z = z_0$ by addition of W (solid contours, from Figure 5a) and A_m (vertical lines), for a particular value of x. W_t is strictly schematic (i.e., not calculated). See text.

in between. But if, for example, $x \simeq -x_1'$, state 2 would disappear and, if $x \simeq -x_2'$, state 1 would disappear.

On the other hand, if $W(x',s)$ at $z = z_0$, $\Delta x = 0$ had more or less the appearance of the contour map in Figure 5b (i.e., the angle θ is very flexible in both states), and if K_L is large, then both attached states would exist in the structured system over almost all of the range $-R \leq x \leq +R$. That is, there would be two minima in $W_t(s)$. Outside of this range of x, the cross-bridge could not reach the site for attachment (since S2 is assumed to be almost inelastic).

Possible Appearance of a New Attached State. As another example, imagine the $A_m(x + x')$ vertical valley in Figure 8 introduced into Figure 6 with $x' = -x$ located at or near the arrow shown on the abscissa. Note that the surface $W(x',s)$ is rather flat in the neighborhood of $s = s_2$, $x' = -x$, and that the two minima in W (states AM_1 and AM_2) are deep and narrow (as functions of x'). Therefore, the function $W_t = W + A_m$, over a certain range of x values, will have *three* minima (corresponding to three attached states) rather than two as in $W(x',s)$: the wells at x_1' and x_2' will not be obliterated (or displaced significantly) by the addition of A_m because these wells are narrow (along x') relative to the curvature of A_m, and sufficiently deep; and a *new* basin will appear in W_t near $s = s_2$, $x' = -x$ because W is rather flat here and A_m itself contributes a minimum (along x').

The three states (minima) are illustrated schematically by the dashed curve W_t in the inset of Figure 6. The curves here are shown as functions of x' along the reaction path.

This phenomenon will arise only if K_L is not too large and if W has at least one rather flat region along the reaction path in W. A case in which it *would* occur is the Huxley-Simmons (1971, 1973) model. Of course, if the rate constants for transitions out of the new state are sufficiently large over the entire range of x involved, then this state would be only a transient intermediate and of no particular consequence.

In the above example, the new attached state occurs with the elastic element at its rest position. Another example, which may have physiological significance, would be the appearance of a new attached state with the elastic element

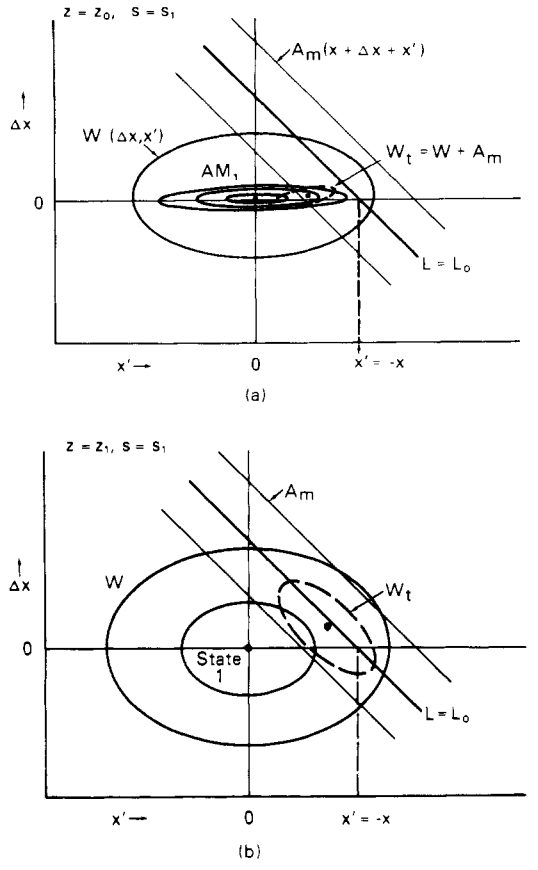

FIGURE 9: (a) The free energies shown at the lower left of Figure 8, with $z = z_0$, are here viewed as functions of Δx and x' with s held constant at $s = s_1$ (state 1). See text for further details. W_t (dashed contour) is strictly schematic. (b) The same example at $z = z_1$. See text.

S2 stretched but with the cross-bridge not quite at a 45° angle to the actin. For example, if we superimpose, in Figure 8, a very narrow and deep well at the AM_2 minimum in $W(x',s)$ (unstructured system), then in the structured system, the basin represented by the dashed curves would be a new state that would occur *in addition* to AM_2 rather than *in place* of it (as is the case in Figure 8 as it stands). This would have physiological significance if the cross-bridge could detach at an appreciable rate only from the deep AM_2 well. In the basin (new state), then, it could exert force but not detach. Of course, if the actin and myosin filaments moved relative to each other so that the elastic element was no longer stretched, it would be easy for the cross-bridge to swing (change θ) from the new basin to the AM_2 well. The rate of detachment would then increase. Thus the presence of a new state of this kind could provide a way of allowing the cross-bridge to detach rapidly only after it had performed work—a fundamental requirement of most cross-bridge models, as pointed out by A. F. Huxley.

Attachment-Detachment Transitions. If the functions $W(\Delta x,z,x',s)$ and $A_m(x + \Delta x + x')$ are available for a given reaction $M_1 \rightleftarrows M_2$ of the myosin cycle, from some assumed model (as in the Figure 8 example above), then the complete reaction free energy surface $W_t = W + A_m$ (for a given x) will of course encompass the attachment-detachment transitions of the structured system [(e) and (e') in Figure 2] as well as the unattached [(a) in Figure 2] and attached [(d) in Figure 2] transitions. We consider an example.

As regards W, to keep the number of independent variables manageable, we fix $s = s_1$ (and thus examine only the state 1 transitions $AM_1 \rightleftarrows A + M_1$) but we allow Δx to vary about $\Delta x = 0$. We can then investigate the function $W(\Delta x,x')$ at several values of z (as we did in Figure 5 with variables x' and s).

Figure 9a represents the same example as in the lower left portion of Figure 8 (state AM_1), but with s replaced by Δx as a variable. The solid contours W indicate again that, at $z = z_0$, state 1 has some flexibility in x' (i.e., in θ) but that the attachment of S1 to the actin site is strong only when Δx is quite small (see Figure 3). The scales of Δx and x' are equal in Figure 9. The value of x chosen is the same as in Figure 8. When $L = L_0$, $\Delta x + x' = -x$. Thus the vertical valley (A_m) in Figure 8 runs at a 45° angle in Figure 9. The dashed contours (W_t) in Figure 9a represents state AM_1 in the structured case ($x' \simeq -x/2$ and $\Delta x \simeq 0$, at the minimum in W_t, in agreement with Figure 8).

Farther out from the actin site, at $z = z_1$, W and W_t might appear as in Figure 9b (A_m is unchanged). The attachment is weak (W) and now quite insensitive to Δx as well as to x' (compare the lower portion of Figure 5b). At $z = z_2$, $W \simeq$ constant (Figure 4b) and only the A_m valley would appear in the corresponding figure (not shown).

Thus, in the attachment process (z decreasing), S1 initially (z large) has the full flexibility of the A_m valley (i.e., θ is free to change), but at $z = z_1$ this flexibility is somewhat reduced (W_t in Figure 9b) by the weak attraction of the site. At $z = z_0$ the site holds $\Delta x \simeq 0$ while the minimum in W_t at $x' \simeq -x/2$ is the result of a compromise between angle bending and S2 compression. In this example $W_t(z)$, along the best path of approach to the actin site, need not exhibit a free energy barrier because the attraction of the actin site helps to compress S2 as $z \rightarrow z_0$. If such a barrier did occur, it would, of course, reduce the rate of attachment. For example, if W in Figure 9a showed a deep narrow well along x' (as in Figure 6; $s = s_1$) as well as along Δx, with a neighboring plateau, then the virtually unaided compression of S2, necessary before the system can fall into the free energy well at $z = z_0$, $\Delta x \simeq 0$, $x' \simeq 0$, would introduce a significant barrier (in W_t) to attachment. In other words, in this case, where the only molecular elasticity is in S2, attachment would be relatively slow because it must wait upon an unaided fluctuation in S2 to the required length.

References

Bagshaw, C. R., Eccleston, J. F., Eckstein, F., Goody, R. S., Gutfreund, H., and Trentham, D. R. (1974), *Biochem. J. 141,* 351.

Eisenberg, E., and Kielley, W. W. (1973), *Cold Spring Harbor Symp. Quant. Biol. 37,* 145.

Hill, T. L. (1956), Statistical Mechanics, New York, N.Y., McGraw-Hill, pp 193, 237.

Hill, T. L. (1960), Statistical Thermodynamics, Reading, Mass., Addison-Wesley, p 313.

Hill, T. L. (1974), *Prog. Biophys. Mol. Biol. 28,* 267.

Hill, T. L. (1975a), *Proc. Natl. Acad. Sci. U.S.A. 72,* 4918.

Hill, T. L. (1975b), *Prog. Biophys. Mol. Biol. 29,* 105.

Hill, T. L. (1976), *Proc. Natl. Acad. Sci. U.S.A. 73* (in press).

Hill, T. L., and Simmons, R. M. (1976), *Proc. Natl. Acad. Sci. U.S.A. 73,* 95, 336.

Huxley, H. E. (1969), *Science 164,* 1356.

Huxley, A. F., and Simmons, R. M. (1971), *Nature (London) 233,* 533.
Huxley, A. F., and Simmons, R. M. (1973), *Cold Spring Harbor Symp. Quant. Biol. 37,* 669.
Lymn, R. W., and Taylor, E. W. (1971), *Biochemistry 10,* 4617.
Moore, P. B., Huxley, H. E., and DeRosier, D. J. (1970), *J. Mol. Biol. 50,* 279.

Effects of Paramagnetic Shift Reagents on the ^{13}C Nuclear Magnetic Resonance Spectra of Egg Phosphatidylcholine Enriched with ^{13}C in the *N*-Methyl Carbons†

Barry Sears,* William C. Hutton,‡ and T. E. Thompson

ABSTRACT: Effects of paramagnetic shift reagents on the ^{13}C NMR spectra obtained from single-walled vesicle dispersions of egg phosphatidylcholine enriched with ^{13}C in the *N*-methyl carbons are investigated. Spectra obtained at 25.1 MHz show that, at Yb^{3+} to phospholipid molar ratios as low as 0.06, complete resolution of the *N*-methyl carbon resonances is obtained from molecules on the inner and outer faces of the vesicle bilayer. No precipitation of the vesicles is caused by Yb^{3+} at these concentrations nor is appreciable line broadening observed. Other paramagnetic shift reagents frequently used in proton NMR investigations of phosphatidylcholine vesicles do not give complete separation of the *N*-methyl ^{13}C signals from the two bilayer surfaces. $K_3Fe(CN)_6$, Eu^{3+}, and Pr^{3+} cause precipitation of the phosphatidylcholine vesicles at concentrations which give only incomplete resolution of these signals. T_1 measurements of the resonances separated by Yb^{3+} indicate that the choline groups on the inner bilayer surface are less mobile than are the same groups in the outer surface. Gated proton decoupling measurements, which show that the nuclear Overhauser effect is 2.8 ± 0.1, indicate that the dominant mode of relaxation is dipolar interaction.

Phospholipid vesicles are generally accepted as useful models for the study of lipid-lipid interactions of the types occurring in biological membranes. Among the physical techniques that may be utilized in such studies, nuclear magnetic resonance (NMR) spectroscopy has proved to be particularly powerful. Two NMR parameters yielding important information are spin-lattice relaxation times (T_1) and chemical shifts produced by paramagnetic shift reagents. The former can be directly related to molecular motion parameters and the latter allow analysis of the distributions of phospholipid molecules on the inner and outer surfaces of vesicles. Although many studies on the phospholipid bilayer system have been carried out using proton and ^{31}P NMR, relatively little work has been done with the ^{13}C nucleus (for a review, see Lee et al., 1974). ^{13}C NMR has several important advantages; the chemical shift range is large compared with ^{1}H and interpretation of the T_1 relaxation data is less complicated. The T_1 times of protonated carbons are dominated by the motions of the intermolecular C-H dipole (Allerhand et al., 1971). With ^{31}P NMR the situation with regard to relaxation times is more complex. Not only are the relaxation times much longer but, in phospholipid vesicles, chemical shift anisotropy makes a significant contribution to the relaxation (Berden et al., 1974). In addition, the relative isolation of the protonated ^{13}C nucleus decreases the perturbation of the chemical shift reagent on the relaxation behavior. However, these advantages of ^{13}C NMR are compromised by the low natural abundance of this nucleus compared with both ^{1}H and ^{31}P. This situation can be greatly improved, however, by synthetic enrichment of ^{13}C at specific locations in the phospholipid molecule. Enrichment markedly increases the sensitivity and in addition simplifies the spectrum to give a single resonance (Sears et al., 1974). In the study reported herein we utilize single-walled vesicles prepared from phosphatidylcholine enriched in the *N*-methyl carbons with ^{13}C (90%) to compare the effectiveness of various paramagnetic shift reagents and determine T_1 values for the *N*-methyl resonances arising from the inner and outer surfaces of the vesicle wall. In addition paramagnetic Yb^{3+} and Pr^{3+} are used to determine the ratio of resonances associated with the outer and inner surfaces of the bilayer comprising the vesicle wall (Sears et al., 1975).

Experimental Section

Preparation of ^{13}C-Enriched Phosphatidylcholine. Phosphatidylcholine enriched in the *N*-methyl carbons with ^{13}C was prepared by the condensation of phosphatidic acid derived from egg phosphatidylcholine with ^{13}C-enriched choline acetate. The [^{13}C]choline was prepared by adding 6.7 mmol of [^{13}C]methyl iodide (Merck, Sharpe and Dohme) to 8 mmol of redistilled 2-dimethylethanolamine (Aldrich) in 20 ml of dry benzene. A precipitate formed immediately.

† From the Department of Biochemistry, University of Virginia School of Medicine, Charlottesville, Virginia 22901. *Received September 5, 1975.* This investigation was supported by U.S. Public Health Service Grant GM-14628. One of us (B.S.) was the recipient of a National Institutes of Health Postdoctoral Fellowship.

* Address correspondence to this author at the Department of Medicine, Boston University School of Medicine, Boston, Massachusetts 02118.
‡ Department of Chemistry, University of Virginia.